IEEE Access
Multidisciplinary ⋮ Rapid Review ⋮ Open Access Journal

Received 7 June 2023, accepted 25 June 2023, date of publication 28 June 2023, date of current version 6 July 2023.

Digital Object Identifier 10.1109/ACCESS.2023.3290553

RESEARCH ARTICLE

Dielectricless Floating-Patch Antenna at 28 GHz Fed With an Empty Substrate Integrated Waveguide

MARCOS D. FERNANDEZ[1], DARÍO HERRAIZ[1], DAVID HERRAIZ[2], AKRAM ALOMAINY[3], (Senior Member, IEEE), AND ANGEL BELENGUER[1], (Senior Member, IEEE)

[1]Departamento de Ingeniería Eléctrica, Electrónica, Automática y Comunicaciones, Escuela Politécnica de Cuenca, Universidad de Castilla-La Mancha, Campus Universitario, 16071 Cuenca, Spain
[2]Instituto de Telecomunicaciones y Aplicaciones Multimedia, Universitat Politècnica de València, 46022 Valencia, Spain
[3]School of Electronic Engineering and Computer Science, Queen Mary University of London, E1 4NS London, U.K.

Corresponding author: Marcos D. Fernandez (marcos.fernandez@uclm.es)

This work was supported in part by Ministerio de Ciencia e Innovación, Spanish Government, through the Subproject C44 of the Coordinated Research and Development Project funded by MCIN/AEI/10.13039/501100011033 under Project PID2019-103982RB and Project TED2021-129196B; and in part by the Funds NextGenerationEU/PRTR.

ABSTRACT This paper presents a novel dielectricless floating patch antenna structure fed with an empty substrate integrated waveguide (ESIW). The main premise is to eliminate the dielectric from the patch design, which is equivalent to have an air-dielectric and leads to the necessity of a proper 3D printed plastic support to fasten the patch in the air above the ESIW, which is used as the feeding waveguide through a slot under the aperture-coupled approximation. A single-element antenna prototype has been studied, designed, optimized and manufactured in order to achieve excellent bandwidth, directivity, gain and beamwidth performance at 28 GHz. The main advantages of this prototype are a low fabrication cost, low losses, a low profile, high integration capability and removal of bulky dielectric material. On the whole, this prototype is a new suitable solution to be used in millimeter-wave 5G applications and beyond compared to the state-of-the-art.

INDEX TERMS Dielectricless, patch, ESIW, 3D printing, 5G.

I. INTRODUCTION

The quick development of wireless communication systems for mass public (i.e. 5G) and the enhancement of the massive use of Internet for almost any device or gadget (i.e. Internet-of-Things – IoT) imply the need of a proper spectrum and bandwidth to allocate those services. A suitable option may be the use of millimeter-wave (MMW) frequency bands to cope with a high data throughput and a wide coverage [1], [2].

In fact, as 5G communication in the high band (above 24 GHz) has finally become a reality,numerous antennas will be required to make these new systems and services work according to their specific characteristics. It is necessary to get low losses, together with high integrability of antennas. Antenna-in-Package (AiP) should be a proper solution to make feasible such mm-wave communication, as integrating the antenna into the packaging substrate reduces the overall interconnect length between radiofrequency integrated circuits and antennas, mitigates the feed-line loss and enhances the antenna efficiency. This solution for 28 to 39 GHz has been mainly used in recent researches and consumer electronics; as a matter of fact, this has been recognized as one of the packaging challenges and mainstream in mm-wave 5G package architecture. Integrated antennas are usually made with patches, but an integrated patch requires an increase in height substrate to improve bandwidth; nevertheless, that height or patch size increase is compensated with performance results [3].

It is proved that miniaturization of patch antennas on a substrate can lower the efficiency due to the excitation of higher-order-mode surface waves at the boundary of air

The associate editor coordinating the review of this manuscript and approving it for publication was Photos Vryonides.

This work is licensed under a Creative Commons Attribution 4.0 License. For more information, see https://creativecommons.org/licenses/by/4.0/

dielectric as well as conductive and dielectric losses; on the other hand, increasing dielectric thickness and permittivity excite higher-order-mode surface waves in the antenna substrate and may reduce antenna efficiency. Hence, a common technique to improve antenna efficiency is the use of air cavities in the substrate to lower the dielectric constant, or even the removal of the dielectric material (equivalent to having air as substrate) provided that a suspended patch could be designed. These solutions would increase the efficiency of the antenna by reducing surface waves and dielectric loss [4].

High-gain, efficiency, low loss and wide bandwidth will be common requirements for the radiating elements, together with a compact size, a low weight and an easy integration with electronic devices [5], [6]. Several designs and approaches are available in the literature [7], [8], [9], [10], [11], [12], [13], [14], [15], [16]; among all of them, the most promising are those based on substrate integration for the feeding section, as this technology accomplishes many of the former features [17].

An optimal selection of the dielectric material and its thickness has little influence on the resonance frequency, but it is of paramount importance to achieve maximum radiation efficiency and bandwidth [18]. On the other hand, as the dielectric constant affects the size of the patch, it could be stated that the higher the dielectric constant, the tinier the patch will be; but, theoretically, the smaller the dielectric constant, the better the antenna performance will be [19]. In fact, in [20], [21], [22], [23], [24], [25], [26], and [27] researchers proved both, theoretically and experimentally, that a floating patch with an air dielectric improves the performance of the bandwidth and gain; however, this is at the cost of a small increase in size. This increase can be minimized by shorting posts and slots at the cost of increasing the manufacturing complexity [28].

Different approaches to the solution of dielectric removal by using air as the separation between the floating patch and the feeding network can be found in several examples reported in the literature. For instance, in [21] two patch antennas for 5G applications at 28 GHz are compared under the same restraints, one based on a dielectric filled substrate integrated waveguide (DFSIW) structure and the other based on air-filled substrate integrated waveguide (AFSIW), where the patch is not floating, but cavity-backed; the results show that the prototype based on AFSIW presents a better performance in efficiency, gain and bandwidth than its DFSIW counterpart. Furthermore, in [22] a cost-effective high-performance antenna is designed by exploiting the low Q-factor of the air cavity formed by an AFSIW feeding and a resonant hourglass-shaped-aperture coupling to a resonant squared patch; it also states that the use of cavities helps minimizing backside radiation. The drawback of this solution is the complexity of the hour-glass aperture and the fact that the patch is not a floating structure. Another example by [23] provides a patch antenna at 28 GHz implemented by 2.5D PCB process where an air-filled cavity-backed is used to improve the performance; the results are promising for a single-element patch antenna, but the manufacturing procedure is quite complicated and the patch is not a floating element. An additional example could be found in [24], where a 1×2 patch array is designed using AFSIW as cavity-backed support to enhance the performance; despite achieving good results, similar performance values could have been achieved by single-element patch antennas and besides, the patch feeding structure is quite large (including a double transition from GCPW to DFSIW and DFSIW to AFSIW).

The former examples of use essentially involve the employment of the cavity-backed technique to substitute the dielectric by air, but the approximation intended in this paper is to make the patch a floating element. For that reason, a support might be needed, and at this point 3D printing solutions can be very helpful. For instance, it is stated in [25] the different manufacturing possibilities to use air as the substrate in high-gain and high-bandwidth antennas and the benefits of considering 3D printing to fabricate hollow structures of substrates with air gaps, which allows a rapid prototyping. In fact, several successful designs are shown, like a 4.5 GHz patch antenna, using a Lego-like 3D printed structure to build air spacers, where the metal parts are made later; nevertheless, despite its feasibility, the procedure described is quite long and complex. Another similar example for an 8.3 GHz patch antenna is included in [26], where once more a Lego-like structure is used, but in this case it also uses a magnetic nanoparticle thin film to help in the manufacturing process, which is still complicated despite the promising results obtained. Eventually, a third example can be cited [27] that makes use of 3D printing structures to implement dielectric parts with backed-cavities of a circularly polarized 3.8 GHz patch antenna with a mix of dielectric and air as substrates. This last solution implements a hybrid approximation, together with shorting-pins, acrylic and metal screws to hold the whole structure, which makes the procedure quite complex to design and implement.

The absence of dielectric in the empty substrate integrated solutions for the feeding section may guarantee a rectangular waveguide (RWG) like behaviour at high frequency, but with a low loss, a low cost and a high integration capability. The solution implemented by the empty substrate integrated waveguide (ESIW) [29] is the one that best emulates a RWG and has already been successfully used to feed MMW antennas made up of slots or non-empty patches [10], [11]. Up to now, the existing proposals for radiating elements using RWG-like feeding networks around 28 GHz are restricted to classical slots and patches with a dielectric material. As previously stated, a lower dielectric constant will produce a better antenna performance. Some approximations, formerly mentioned, have tried to implement this fact using partially emptied waveguides (like AFSIW) and making use of the cavity-backed technique, but none has been done using an ESIW at that frequency and implementing a floating patch instead of a cavity-backed patch. That is precisely

the goal of this paper: to prove if a floating patch antenna (with air-dielectric) can be developed at 28 GHz using an ESIW for the feeding section. A totally novel approach has been considered in a prototype based on an ESIW as the feeding line, which excites the patch through a slot (aperture-coupled) cut in the upper layer of the ESIW and uses air as the dielectric for the floating patch, which is fixed to the ESIW structure with a plastic 3D-printed frame. This paper proves the feasibility of this approach and shows, for the first time, the manufacture of such prototype and its measurement.

II. DESIGN GOALS AND PROCEDURE

The proposed antenna, to be fabricated as a proof-of-concept of feasibility, will radiate at 28 GHz, with around 1 GHz bandwidth and 8 dBi directivity, through a floating metallic thin patch with h_{air} mm of air-dielectric ($\epsilon_r = 1$) between the patch and the ground plane. As restraints, the following are imposed: an empty planar waveguide (an ESIW) will be used in the feeding section; the device will be a PCB-based multilayered structure consisting of a combination of different thickness substrates (Rogers-4003C, $\epsilon_r = 3.55$, $\tan\delta = 0.0027$, 17.5 μm cladding thickness by each side); the patch will be also a piece of 0.203 mm thickness substrate with the edges metallized with an electrodeposition of 9 μm of copper; and a proper fastener will be needed to stabilize the position of the floating patch.

The well-known design equations for a microstrip patch included in [19] and summarized in [12] will be used to calculate the initial values for the patch size; for a chosen radiation frequency of f_r GHz and the air as the patch dielectric ($\epsilon_{r_{eff}} = \epsilon_{r_{air}} = 1$), the design equations for the patch are simplified as follows:

$$W_p = \frac{c}{2f_r} \tag{1}$$

$$\Delta L = 0.722 \cdot h_{air} \frac{0.264 + \frac{W_p}{h_{air}}}{0.8 + \frac{W_p}{h_{air}}} \tag{2}$$

$$L_p = \frac{c}{2f_r} - 2\Delta L \tag{3}$$

where W_p is the size of the radiating edges (y axis), L_p is the size of the non-radiating edges (x axis), $\epsilon_{r_{eff}}$ is the effective dielectric constant (that matches to $\epsilon_{r_{air}} = 1$ in this case) and ΔL is the correction in size due to the fringing effects on the patch. As the structure to use in the proposals of this paper is not the standard microstrip patch antenna commonly described in the bibliography, the equations used give only an initial approximation of the dimensions; then, the device will be modelled and numerically evaluated using CST Studio Suite through optimization algorithms to obtain the final dimensions.

This prototype is made up of three parts: an ESIW fed with a tapered transition from a microstrip line and ended in a short-circuit, a slot cut in the upper layer of the ESIW at a distance to the short-circuit that maximizes the radiation, and a floating patch antenna optimized to radiate at 28 GHz and fastened with a plastic support to the device. The appearance and design parameters are illustrated in Fig. 1, where three different views of the proposed designs are shown to appreciate the inner details of the device and its parts and dimensions. This design structure has been chosen to combine the proper conditions of each separate part that can empower the final design of a real floating patch antenna (non cavity-backed) fed with a planar waveguide: the ESIW is the planar waveguide most similar to a RWG, the slot feeding minimizes the backward radiation of the patch and improves maximum radiation if it is correctly positioned in the waveguide, the air substrate helps in the achievement of better antenna performance, and the plastic support integrates practical 3D printing solutions into the design with minimal electromagnetic impact. This combination is feasible, cost-efficient and easy to manufacture.

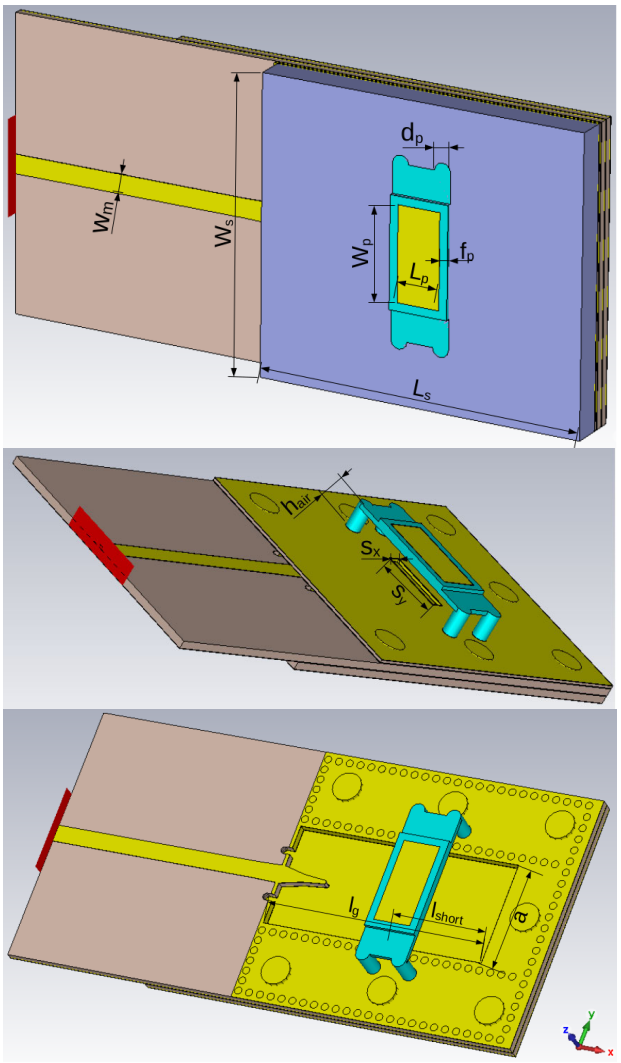

FIGURE 1. Appearance and design parameters of the empty-patch ESIW-fed prototype. From top to bottom: top view of the device [included dimensions w_m, W_s, L_s, W_p, L_p, d_p, f_p], view removing the top layer and the air layer [included dimensions s_x, s_y, h_{air}], view of the layer that includes the microstrip line [included dimensions a, l_g, l_{short}]. Color legend: light brown is substrate, light blue is plastic (ASA), yellow is copper, purple is air and background gray/white is air, red is the input port.

The ESIW section, built according to [29], is composed of three layers: bottom and middle layers are Rogers-4003C of thickness 0.508 mm, whereas top layer is Rogers-4003C of thickness 0.203 mm. The middle layer includes a microstrip line to inject the power through an exponential taper transition into the ESIW, whose width ($a = 7.112$ mm) is equivalent to a standard Ka-band rectangular waveguide (WR-28); the other end of the ESIW is a short-circuit.

The aperture-coupled approximation has been adopted to feed the patch antenna; for that, the top layer of the ESIW has a transverse slot, of size $s_x \times s_y$, (centered along the width of the ESIW) at a distance l_{short} of the ESIW short-circuit conveniently optimized to a maximum radiation. Initial values of the slot size and position, according to [30], are estimated to be positioned at the peak of the standing waves profile in order to excite the patch at maximum coupling and aligned with the center of the patch (initially $s_x = 1$ mm, $s_y = 2.2$ mm, $l_{short} = 7.6$ mm).

The patch is just a piece of Rogers-4003C of thickness 0.203 mm, completely metallized, of size $L_p \times W_p$ at a distance h_{air} over the slot. To begin with, the patch is calculated according to [12] for an arbitrary value of h_{air} (initially $h_{air} = 1.504$ mm, $W_p = 5.353$ mm, $L_p = 3.449$ mm); later these three values have been optimized to obtain the maximum radiation at 28 GHz.

Once fixed the value of h_{air}, an ASA-plastic structure has been designed to support and fasten the floating patch, so that it can be inserted into the upper layer of the ESIW maintaining the optimum distance of h_{air}. That fastener includes a thin perimetral frame to secure the insertion and position of the patch, as well as four posts to be inserted within the top layer of the ESIW to ensure the position of the plastic support; structure and dimensions of the fastener have been considered to be the minimum possible so that it could be relatively easy to manipulate, but with the minimum interference in the radiation. Therefore, this plastic structure, before being manufactured with a professional 3D-printer, has been included in the simulations to check that it does not interfere considerably in the prototype performance; in fact, its effect can reduce the antenna gain up to 1 dB, and consequently, the final optimization of the whole device, essentially the size of the patch ($L_p \times W_p$), is done including the plastic support.

The design procedure for the ESIW-fed prototype can be summarized as follows (considering also the dimensions to be determined at each stage):

1) Design of the microstrip and ESIW sections ($h_1, h_2, w_m, W_s, L_s, l_g$).
2) Design and optimization of the size and position of the slot in the top layer of the ESIW (l_{short}, s_x, s_y).
3) Design and optimization of the patch size and distance between the patch and the top layer of the ESIW (h_{air}, L_p, W_p).
4) Design of the plastic fastener to support the floating patch (d_p, f_p).
5) Final optimization process of the patch size (L_p, W_p).

Because of the importance of the second and third design steps, a parametric study has been conducted on the influence of each parameter, around their quasi-optimum values, in the performance value of S_{11}. The position of the slot (l_{short}) considerably affects to resonance frequency and return loss; however, it is an easily adjustable parameter and it can be accurately implemented. The size of the slot (s_x, s_y) has little influence on the return loss and its s_y dimension also shifts slightly the resonance frequency. The influence of the dimension W_p of the patch is negligible in comparison with the other variables considered, whereas the L_p dimension (distance between the radiating edges) does really affect to the return loss and, with minor importance, to the resonance frequency. The size of the slot and patch can be accurately manufactured. The dimension with the most sensitive influence is the height h_{air} that separates the patch from the slot, as it affects heavily to resonance frequency, return loss and bandwidth. This dimension is controlled through the height of the 3D-printed plastic support made with a 3D printer; therefore, the accuracy of the 3D printer will be of paramount importance. Fig. 2 shows the effects of the most critical dimensions according to the parametric analysis described.

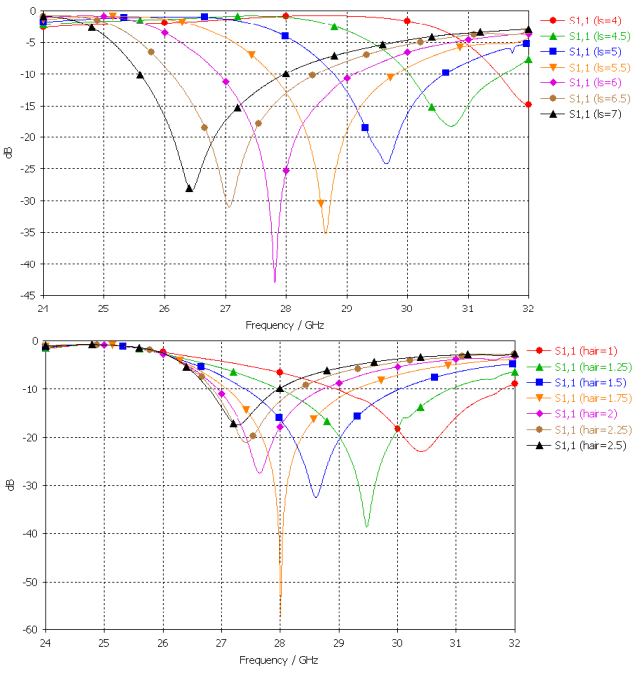

FIGURE 2. Variation of S_{11} according to a parametric analysis of: l_{short}, position of the slot (top), and h_{air}, separation between the patch and the slot (bottom).

After the last optimization process of the fifth design step, the final dimensions of the prototype are those of table 1. Simulation of this device (with losses and plastic support) indicates that the antenna will fit the requirements established. In particular, simulations foresee a device with 5% bandwidth around 28 GHz, with a directivity of 8.3 dBi and a total efficiency of 93%.

TABLE 1. Optimum dimensions (in *mm*) for the floating patch device.

h_1	h_2	h_{air}	w_m	d_p	f_p	l_{short}
0.508	0.203	1.756	1.174	1	0.5	5.881
W_s	L_s	W_p	L_p	s_x	s_y	l_g
18	20	5.764	2.604	0.826	4.631	15.890

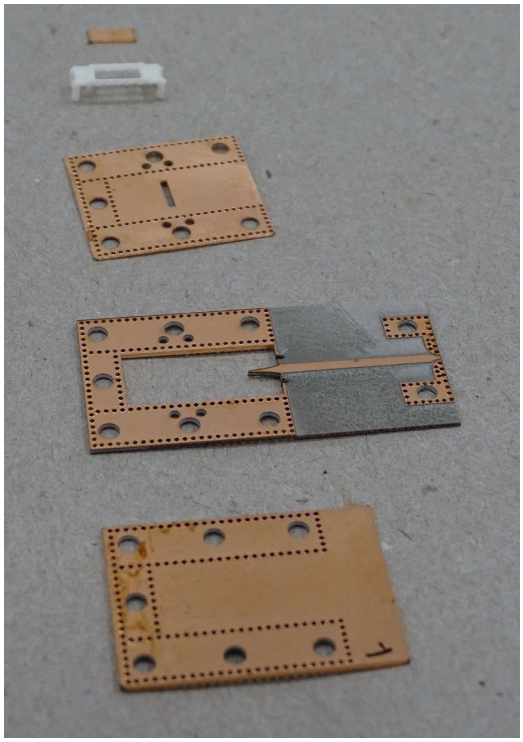

FIGURE 3. Pieces, from top to bottom, to build up the prototype: patch, supporting frame, top layer, central layer and bottom layer.

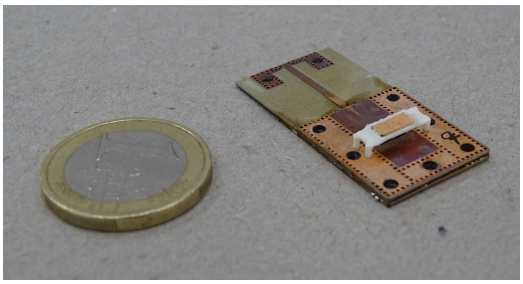

FIGURE 4. Manufactured prototype with a 1 euro reference scale.

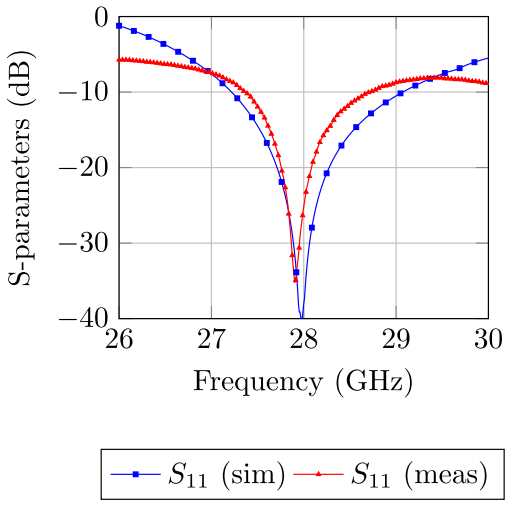

FIGURE 5. Measured and simulated results for the parameter S_{11}.

III. EXPERIMENTAL EVALUATION RESULTS AND ANALYSES

The designed device has been manufactured and the resulting prototype is that shown in Fig. 3, where the different pieces that must be properly assembled are shown; and Fig. 4, which compares the size of the whole prototype with a 1 euro coin. The manufacturing process is quite simple and can be done with standard PCB operations, such as drilling, cutting, milling, plating and soldering; for the plastic suppport a specific design is printed with a professional 3D plastic printer of 127 μm accuracy in the z-axis. Once the ESIW is built, the fastener is inserted in the proper holes drilled in the top layer, and then the patch is placed in the frame of the support with a little drop of contact-glue. The accuracy in the fastener manufacturing is of paramount importance, as it is responsible of controlling the exact separation distance h_{air} between the slot and the patch (for that, the length of the fastener posts is enlarged adding the depth to be inserted in the top layer), as well as the correct orientation of the patch (this is solved with the thin frame to ensure the placement of the patch).

Losses from the microstrip section have been experimentally measured with a thru element specifically designed for that purpose. The microstrip losses are 1.0 dB and do not include the ESIW transition. Those losses will be removed to properly characterize the antenna performance, but the results will still be a pessimistic approximation, as losses due to the ESIW transition have not been removed. Considering the former, the prototype has been measured with a vector network analyzer (Agilent N5230C) to characterize the S_{11} parameter. The measured and lossy simulated results are shown in Fig. 5. Differences with the simulation are due to possible manufacturing misalignments (especially those due to 3D printing), copper real losses and surface rugosity. Despite that, the measurement fits quite precisely with the simulation for the band of interest and reflects a measured bandwidth of nearly 1.35 GHz (around 4.8%) with measured return loss of 35 dB at 27.90 GHz; therefore, the design requirements imposed in this proof-of-concept have been fully satisfied.

Radiation of the prototype patch antenna has been also measured in an anechoic chamber with the technique of the reference antenna (Flann22240 in this case), as it can be seen in Fig. 6. With the data acquired in this measurement procedure, the antenna can be completely characterized.

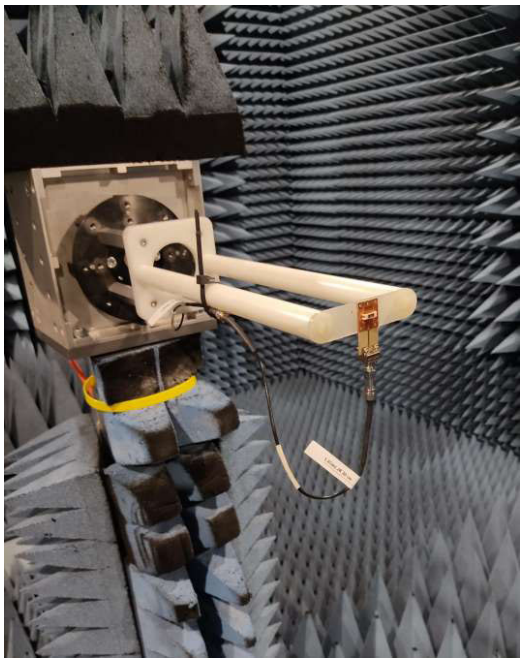

FIGURE 6. Measurement of the prototype in an anechoic chamber with the reference antenna technique.

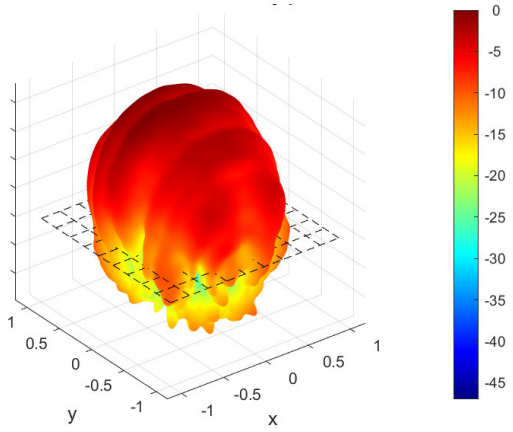

FIGURE 7. 3D representation of measured electric field radiation (normalized, in dB).

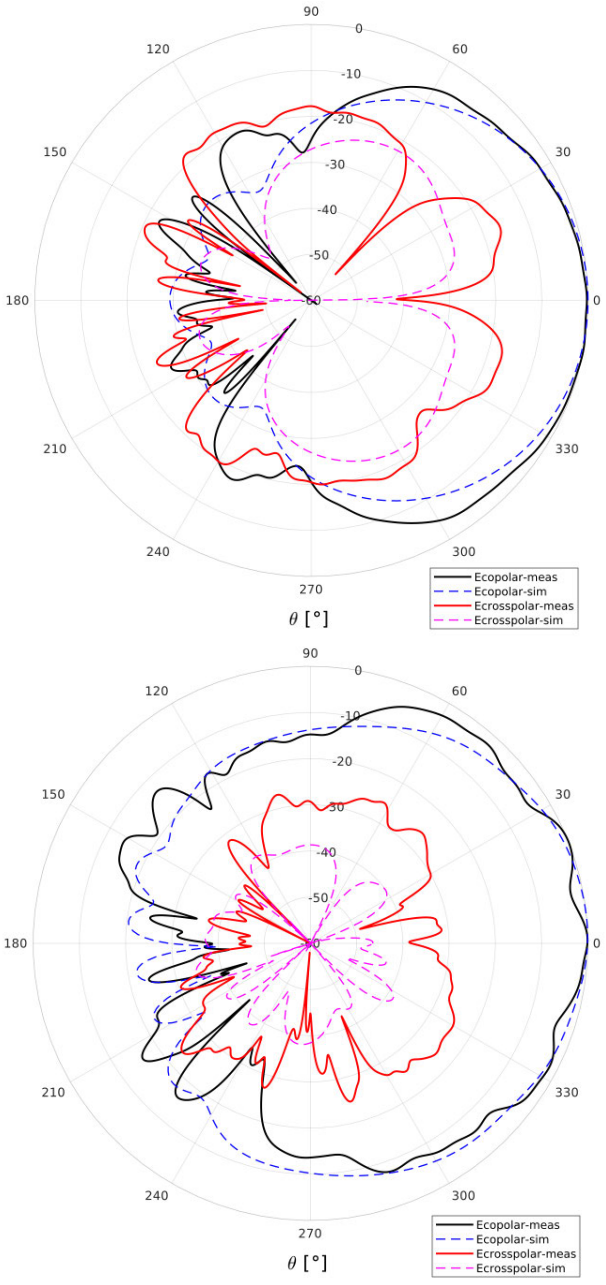

FIGURE 8. Polar-plot cuts of measured and simulated co-polar and cross-polar electric field radiation (normalized, in dB). From top to bottom: plane XZ and plane YZ.

Measured 3D normalized radiation pattern is shown in Fig. 7, whose measured and simulated co-polar and cross-polar XZ and YZ plane cuts are included in Fig. 8. The obtained patterns are typical of a patch antenna with low backward radiation. Normalized simulated and measured copolar radiation are very similar, whereas the measured crosspolar radiation is slightly higher than the simulated one. The measured directivity at the resonance frequency is 8.1 dBi, whereas the measured realized gain is 7.5 dBi and the measured efficiency is 92%. The maximum direction of radiation is at $\theta = 11°$ and $\phi = 181°$, whereas -3 dB beamwidth is practically 60° for plane YZ and 60° for the XZ, and the front-to-back ratio is better than 20 dB. Besides, a good cross-polar rejection of 17 dB is obtained, with 38 dB of polarization ellipse axial ratio.

Those results fit in properly with the simulations and the goals established in the design stage, considering the multiple manufacturing isssues at the frequency of interest, and reveal, as intended, good performance indexes of return loss, bandwidth, beamwidth and directivity simultaneously. The results obtained for that prototype validate the feasibility of the intended proof-of-concept of manufacturing, for the first time, a dielectricless floating patch fed with an ESIW at 28 GHz.

TABLE 2. Comparison with other non-conventional patch antennas. [A-C, aperture-coupled; ACB, air cavity-backed; PS, plastic support; 3DPS, 3D printed substrate].

Ref.	f_r (GHz)	R_L (dB)	BW (%)	G (dBi)	η (%)	Feeding	Manufacturing complexity	Comments
[25]	4.5	20	4.4	7.3	—	coax	complex	3DPS, ACB
[27]	3.65	25	3	10	—	coax	very complex	3DPS, ACB
[26]	7.8	30	4.3	7	—	mstrip	complex	3DPS, ACB
[4]	60	23	12.5	18.6	90	A-C, mstrip	very complex	air, PS, 5x5 array only simulation
[20]	28	20	18	7	85	slot, AFSIW	complex	ACB, dual-resonance dual-polarized
[21]	28	40	3.5	5.8	92	slot, AFSIW	easy	ACB only simulation
[22]	26.88	13.3	26	7.4	85	A-C, AFSIW	complex	ACB, hour-glass slot dual-resonance high back radiation
[23]	28.5	28	3.8	8.7	93	microstrip	complex	ACB, 2.5D PCB only simulation
[24]	28.16	18	7.5	9.8	92	A-C, AFSIW	easy double transition	ACB, 1x2 array dual-resonance only simulation
This	**27.90**	**35**	**4.8**	**7.5**	**92**	**A-C, ESIW**	**easy**	**air, PS**

Inevitably, some inherent fabrication errors might occur during the manufacturing process. A yield analysis has been done in order to validate the repeatability of the process and its endurance, taking into account that errors may appear in the most critical operations: the cutting process for the size of the patch (L_p, W_p) and the slot (s_x, s_y), the positioning of the slot (l_{short}) and the height (h_{air}) of the 3D frame that supports the patch. The two criteria simultaneously selected which must be accomplished to mark a device as acceptable are that $S_{11} < -10\,dB$ at the band between 27.25 GHz and 28.75 GHz and, at least, $S_{11} < -20\,dB$ around the resonance frequency (between 27.90 GHz and 28.10 GHz). Taking into account that the tolerance of the laser cut used is 2 microns, the analysis indicates that even for high tolerances of 25 microns in all the variables analyzed (except h_{air}), the 99.9% of the devices would be acceptable. If tolerance were extremely high, for instance 50 microns, the 95.3% of the prototypes would be acceptable. The 3D plastic printer used to make the support has an accuracy of 127 μm and this essentially affects to the h_{air} parameter; taking only into account 127 micron tolerance error of the 3D printer, the 99.3% of the prototypes would be correct, and with a tolerance higher than 150 microns, even the 95.0% of the prototypes would still be acceptable. Even in the worst case of simultaneous high values of tolerance (50 microns in the laser cut and 150 microns in the 3D printer) the 90.1% of the manufactured prototypes would accomplish the strict fabrication performance criteria imposed. This reveals the accuracy of the design and the high tolerance to manufacturing errors of this prototype.

As this device implements a real dielectricless floating patch at 28 GHz, the comparison with other works available in the literature is quite heterogeneous, as the vast majority of similar devices are whether non-air-dielectric or based on the air cavity-backed technique (many of them using AFSIW); furthermore, many resembling devices are non-single-element antennas (arrays), which, in fact, makes the comparison even more difficult, as arrays usually present a wider bandwidth and a higher gain than single element antennas. Nevertheless, the device presented in this paper, for a single-element antenna, achieves results that emulate, or even improve, other slot, dielectric and cavity-backed patch and array devices, as it is shown in Table 2. For instance, references [25], [26], [27] deal with devices built with 3D printing techniques and air cavity-backed to improve the performance, but all of them at a relatively low frequency (among 3 to 8 GHz) and with no mention about their efficiency. The device presented in this paper is made at 28 GHz, using also a 3D partial solution, but due to its high frequency, the dimensions are quite small and the fabrication tolerances may be an issue; in spite of that, this new device achieves similar measured results in return loss, bandwidth and gain at a much higher frequency, with a simpler manufacturing procedure and with a 92% efficiency. On the other hand, in [4] a 60 GHz floating patch array is presented, with very good performance results according to the simulations (no measurements are shown) if a very complex manufacture procedure, consisting in 25 floating patches (using tiny holding posts) disposed in a 5 $\times$ 5 array, were followed to make the prototype. The device presented in this paper, manufactured and measured, is much simpler to fabricate and achieves very good performance results for a single-element patch. Some prototypes around 28 GHz are also proposed in [20], [21], [22], [23], and [24] (almost all of them based on AFSIW to implement an air cavity-backed). All but two present only simulation results, consequently making the comparison a bit odd, as the simulations results are usually much better than the measured ones; taking that into account, the prototype presented in this paper is, on the whole, similar or even better, than the other devices at 28 GHz. Regarding the return loss, only one design is better, but just with simulated results; if our simulated return loss was considered (40 dB), it would be the best design. The bandwidth of dual-resonance designs is

very high, but our design is not dual-resonance, and within the non-dual-resonance subgroup, our design is the best, as it achieves a 4.8% measured bandwidth and the others are below 4% of the simulated bandwidth. As for the gain and efficiency, our proposal gets 7.5 dBi and 92% respectively, similar to the results of the others, except for [24], which is in fact a 1 × 2 array and only shows simulated results, and [23], which has a narrower bandwidth with a complex manufacturing procedure to implement an air cavity-backed with a non-dielectricless floating patch. Regarding the manufacturing complexity, our proposal is the simplest one; just two other designs could be close to our device's manufacturing easiness, but they do not implement a real dielectricless floating patch and only simulated results are given. All in all, considering the heterogeneity of the comparison, the prototype presented in this paper is really a promising design to implement a real dielectricless floating patch, being fed for the first time with an ESIW, which achieves simultaneously good values in all the measured performance parameters.

IV. CONCLUSION

The paper presented a novel prototype of a dielectricless floating patch antenna fed with a slot from an ESIW and using a 3D-printed fastener to fix the patch for the first time in the open literature. Experimental results based on the fabricated prototype are promising, as it achieves 8.1 dBi directivity and 7.5 dBi realized gain at 28 GHz with more than 1.3 GHz bandwidth. The design procedure requires two essential adjustments: the size and position of the slot in the ESIW, and the size and position of the patch over the ESIW. The design of the plastic fastener is not so trivial, as it needs to be resistant, but the tiniest possible not to affect the radiation. In fact, the most critical aspect is the positioning of fastener and patch. Thanks to the feeding system through a slot in an ESIW, this anntena presents a high integration capability with other planar circuits; at the same time, this device is low-cost, light-weight and robust. Good values in all the performance parameters for a single-element antenna, easiness of design and manufacture, the total absence of dielectric and the use of an ESIW to feed a real dielectricless floating patch present clearly the novelty of the design and original contributions to the field for a promising candidate to be applied in wireless and 5G applications in the 28 GHz band.

REFERENCES

[1] J. G. Andrews, S. Buzzi, W. Choi, S. V. Hanly, A. Lozano, A. C. K. Soong, and J. C. Zhang, "What will 5G be?" *IEEE J. Sel. Areas Commun.*, vol. 32, no. 6, pp. 1065–1082, Jun. 2014.

[2] T. S. Rappaport, S. Sun, R. Mayzus, H. Zhao, Y. Azar, K. Wang, G. N. Wong, J. K. Schulz, M. Samimi, and F. Gutierrez, "Millimeter wave mobile communications for 5G cellular: It will work!" *IEEE Access*, vol. 1, pp. 335–349, 2013.

[3] A. O. Watanabe, M. Ali, S. Y. B. Sayeed, R. R. Tummala, and M. R. Pulugurtha, "A review of 5G front-end systems package integration," *IEEE Trans. Compon., Packag., Manuf. Technol.*, vol. 11, no. 1, pp. 118–133, Jan. 2021.

[4] K. Keshtkaran and N. Ghalichechian, "Suspended 60 GHz phased array antenna with high efficiency," in *Proc. Int. Workshop Antenna Technol. (iWAT)*, Feb. 2016, pp. 37–39.

[5] M. Shafi, A. F. Molisch, P. J. Smith, T. Haustein, P. Zhu, P. De Silva, F. Tufvesson, A. Benjebbour, and G. Wunder, "5G: A tutorial overview of standards, trials, challenges, deployment, and practice," *IEEE J. Sel. Areas Commun.*, vol. 35, no. 6, pp. 1201–1221, Jun. 2017.

[6] R. Mittra, "Some challenges in millimeter wave antenna designs for 5G," in *Proc. Int. Symp. Antennas Propag. (ISAP)*, Oct. 2018, pp. 1–2.

[7] M. Adhikary, S. Mukherjee, A. Biswas, and M. J. Akhtar, "Air filled substrate integrated waveguide cavity backed slot antenna," *Microw. Opt. Technol. Lett.*, vol. 60, no. 11, pp. 2605–2608, Nov. 2018.

[8] O. Darboe, F. Manene, and D. Konditi, "A 28 GHz rectangular microstrip patch antenna for 5G applications," *Int. J. Eng. Res. Technol.*, vol. 12, pp. 854–857, Jun. 2019.

[9] Z. Qi, X. Li, J. Xiao, and H. Zhu, "Low-cost empty substrate integrated waveguide slot arrays for millimeter-wave applications," *IEEE Antennas Wireless Propag. Lett.*, vol. 18, no. 5, pp. 1021–1025, May 2019.

[10] Z. U. Khan, A. Alomainy, and T. H. Loh, "Empty substrate integrated waveguide planar slot antenna array for 5G wireless systems," in *Proc. IEEE Int. Symp. Antennas Propag. USNC-URSI Radio Sci. Meeting*, Jul. 2019, pp. 1417–1418.

[11] Z. U. Khan, T. H. Loh, A. Belenguer, and A. Alomainy, "Empty substrate-integrated waveguide-fed patch antenna array for 5G millimeter-wave communication systems," *IEEE Antennas Wireless Propag. Lett.*, vol. 19, no. 5, pp. 776–780, May 2020.

[12] R. Przesmycki, M. Bugaj, and L. Nowosielski, "Broadband microstrip antenna for 5G wireless systems operating at 28 GHz," *Electronics*, vol. 10, no. 1, Dec. 2020.

[13] W. Tan, Y. Xiao, C. Li, K. Zhu, H. Luo, and H. Sun, "A wide-band high-efficiency hybrid-feed antenna array for mm-wave wireless systems," *Electronics*, vol. 10, no. 19, p. 2383, Sep. 2021.

[14] M. Gemeda, K. Fante, H. Goshu, and A. Goshu, "Design and analysis of a 28 GHz microstrip patch antenna for 5G communication systems," *Int. Reasearch J. Eng. Technol.*, vol. 8, no. 2, pp. 881–886, 2021.

[15] Z. Qi, X. Li, and H. Zhu, "Low-cost high-order-mode cavity backed slot array antenna using empty substrate integrated waveguide for the 5G n260 band," *Frontiers Inf. Technol. Electron. Eng.*, vol. 22, no. 4, pp. 609–614, Apr. 2021.

[16] L. Li and J.-B. Yan, "A low-cost and efficient microstrip-fed air-substrate-integrated waveguide slot array," *Electronics*, vol. 10, no. 3, p. 338, Feb. 2021.

[17] M. Bozzi, A. Georgiadis, and K. Wu, "Review of substrate-integrated waveguide circuits and antennas," *IET Microw. Antennas Propag.*, vol. 5, no. 8, pp. 909–920, Jun. 2011.

[18] A. S. B. Mohammed, S. Kamal, M. F. B. Ain, R. Hussin, F. Najmi, S. A. S. Suandi, Z. A. Ahmad, U. Ullah, M. F. B. M. Omar, and M. Othman, "Mathematical model on the effects of conductor thickness on the centre frequency at 28 GHz for the performance of microstrip patch antenna using air substrate for 5G application," *Alexandria Eng. J.*, vol. 60, no. 6, pp. 5265–5273, Dec. 2021.

[19] C. A. Balanis, *Antenna Theory: Analysis and Design*. Hoboken, NJ, USA: Wiley, 2016.

[20] K. Y. Kapusuz, S. Lemey, and H. Rogier, "Dual-polarized 28-GHz air-filled SIW phased antenna array for next-generation cellular systems," in *Proc. IEEE Int. Symp. Phased Array Syst. Technol. (PAST)*, Oct. 2019, pp. 1–6.

[21] J. Zhang, Y. Duroc, A. Ghiotto, K. Wu, and T. Vuong, "Air-filled substrate integrated waveguide (AFSIW) cavity-backed slot antenna for 5G applications," in *Proc. IEEE Int. Symp. Antennas Propag. North Amer. Radio Sci. Meeting*, Jul. 2020, pp. 395–396.

[22] I. L. de Paula, S. Lemey, D. Bosman, Q. V. D. Brande, O. Caytan, J. Lambrecht, M. Cauwe, G. Torfs, and H. Rogier, "Cost-effective high-performance air-filled SIW antenna array for the global 5G 26 GHz and 28 GHz bands," *IEEE Antennas Wireless Propag. Lett.*, vol. 20, no. 2, pp. 194–198, Feb. 2021.

[23] H. Takahashi, S. W. Sattler, E. Schlaffer, B. Reitmaier, H. Sarbandifarahani, H. Paulitsch, and W. Bösch, "Air-filled cavity-backed 28 GHz antenna array implemented by 2.5D PCB process and network analysis," in *Proc. 51st Eur. Microw. Conf. (EuMC)*, Apr. 2022, pp. 534–537.

[24] N. Nguyen, A. Ghiotto, M. T. Le, and T. Vuong, "High gain microstrip patch antenna array using air-filled substrate integrated waveguide (AFSIW) feeding structure," in *Proc. Int. Conf. Adv. Technol. Commun. (ATC)*, Oct. 2022, pp. 54–57.

[25] M. I. M. Ghazali, S. Karuppuswami, A. Kaur, and P. Chahal, "3-D printed air substrates for the design and fabrication of RF components," *IEEE Trans. Compon., Packag., Manuf. Technol.*, vol. 7, no. 6, pp. 982–989, Jun. 2017.
[26] Y. He, J. Papapolymerou, E. Drew, and Z. J. Zhang, "Compact microstrip patch antenna utilizing low cost solution cast nanomagnetic thin film," in *Proc. IEEE Int. Symp. Antennas Propag. USNC-URSI Radio Sci. Meeting*, Jul. 2019, pp. 1531–1532.
[27] S. Wang, L. Zhu, J. Wang, W. Wang, and W. Wu, "3-D printing and CNC machining technologies for exploration of circularly polarized patch antenna with enhanced gain," *IEEE Trans. Compon., Packag., Manuf. Technol.*, vol. 9, no. 5, pp. 984–990, May 2019.
[28] S. B. Belamgi and S. Ray, "A compact suspended planar patch antenna for microwave imaging sensor array," in *Proc. 3rd Int. Conf. Comput., Commun., Control Inf. Technol. (CIT)*, Feb. 2015, pp. 1–4.
[29] A. Belenguer, H. Esteban, and V. E. Boria, "Novel empty substrate integrated waveguide for high-performance microwave integrated circuits," *IEEE Trans. Microw. Theory Techn.*, vol. 62, no. 4, pp. 832–839, Apr. 2014.
[30] Z. U. Khan, S. F. Jilani, A. Belenguer, T. H. Loh, and A. Alomainy, "Empty substrate integrated waveguide-fed MMW aperture-coupled patch antenna for 5G applications," in *Proc. 12th Eur. Conf. Antennas Propag. (EuCAP)*, Apr. 2018, pp. 1–3.

MARCOS D. FERNANDEZ received the degree in telecommunications engineering from Universitat Politècnica de Catalunya (UPC), Spain, in 1996, and the Ph.D. degree from Universidad Politécnica de Madrid (UPM), in 2006. He joined Universidad de Castilla-La Mancha, in 2000, where he is currently a Professor Titular de Universidad with Departamento de Ingeniería Eléctrica, Electrónica, Automática y Comunicaciones, and the Dean of Escuela Politécnica de Cuenca. He has authored or coauthored several papers in peer-reviewed international journals and conference proceedings. His research interest includes empty substrate integrated waveguide (ESIW) devices and their manufacturing and applications.

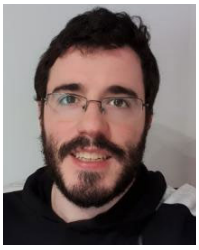

DARÍO HERRAIZ received the Graduate and master's degrees in telecommunications engineering from Universidad de Castilla-La Mancha (UCLM), Spain, in 2019 and 2022, respectively, where he is currently pursuing the Ph.D. degree in telecommunications engineering. He joined Grupo de Aplicaciones de Microondas y Milimétricas, y Antenas (GAMMA Group), UCLM, in 2018, for six months with a research grant, then, in 2019, as a Researcher, and again, in 2021, also as a Researcher. His final degree project is about ESIW and was prized, in 2020, with a national prize from Colegio Oficial/Asociación de Graduados e Ingenieros Técnicos de Telecomunicación (COITT/AEGITT). He has coauthored three articles so far.

DAVID HERRAIZ received the B.Sc. and M.Sc. degrees in telecommunications engineering and the B.Sc. degree in industrial engineering from Universitat Politècnica de Valencia (UPV), in 2018 and 2020, respectively, where he is currently pursuing the Ph.D. degree in telecommunications engineering. From 2020 to 2021, he was a Service Engineer with 5G Communications for Future Industry Verticals (Fivecomm), where he was involved in 5G robotics solutions in several European projects under Horizon Europe, as a ROS Developer and an Applications Integrator with Automated Guided Vehicles (AGVs) and other project management and execution tasks. In 2021, he joined the Institute of Telecommunications and Multimedia Applications (iTEAM), UPV. His current research interests include wideband transition structures, ridge waveguides, additive manufacturing and design, implementation, and the optimization of communication devices in empty substrate integrated technologies and their applications. In 2020, he was a recipient of the COIT-AEIT, Colegio Oficial de Ingenieros de Telecomunicación (COIT), and the Asociación Española de Ingenieros de Telecomunicación (AEIT) in collaboration with HISPASAT Spanish satellite communications operator for his master's degree final project as emerging technologies for Communication Satellite Payloads Award.

AKRAM ALOMAINY (Senior Member, IEEE) is currently the Deputy Dean of Postgraduate Research with the Faculty of Science and Engineering, the Head of the Antennas and Electromagnetics Research Group, and a Reader in antennas and applied EM with the Queen Mary University of London (QMUL). He is also the Lead of Wearable Technology and Creativity Research. Research portfolio ranging from the basics of antennas and electromagnetism to novel applications in telerobotics, cognitive radio, wearable electronics, nano-scale networks, healthcare, and bioenigneering. He has over 450 publications in leading journals and international conferences (more than 10000 citations and H-index of 46). He is also a member of the Centre for Intelligent Sensing and Institute of Bioengineering. He is also a Chartered Engineer of IEEE and a member of IET. He was a recipient of the 2011 British Science Festival Isambard Kingdom Brunel Award and a recipient of the QMUL Education Excellence Award, in 2019. He is also an Associate Editor of IEEE Antennas and Wireless Propagation Letters and IEEE Journal of Electromagnetics, RF and Microwaves in Medicine and Biology.

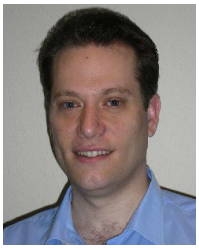

ANGEL BELENGUER (Senior Member, IEEE) received the degree in telecommunications engineering and the Ph.D. degree from Universidad Politécnica de Valencia (UPV), Spain, in 2000 and 2009, respectively. He joined Universidad de Castilla-La Mancha, in 2000, where he is currently a Professor Titular de Universidad with Departamento de Ingenieria Electrica, Electronica, Automatica y Comunicaciones. He has authored or coauthored more than 50 papers in peer-reviewed international journals and conference proceedings. His research interests include methods in the frequency domain for the full-wave analysis of open-space and substrate integrated waveguide (SIW) devices and their applications.